Physico-Chemical Investigation of the State of Cyanamide Confined in AOT and Lecithin Reversed Micelles

P. Calandra,[†] A. Longo,[‡] A. Ruggirello,[†] and V. Turco Liveri*[,†]

Dipartimento di Chimica-Fisica, Università degli Studi di Palermo, Viale delle Scienze Parco d'Orleans II, 90128 Palermo, Italy, and ISMN, Istituto per lo Studio dei Materiali Nanostrutturati, Via Ugo La Malfa 153, 90146 Palermo, Italy

Received: February 19, 2004; In Final Form: March 31, 2004

Sodium bis(2-ethylhexyl)sulfosuccinate (AOT) and lecithin reversed micelles containing cyanamide have been investigated by small-angle X-ray scattering, FT-IR, and ^{1}H NMR spectroscopy at various cyanamide-to-surfactant molar ratio (X) and at fixed surfactant concentration (0.1 mol kg^{-1}). Experimental data are consistent with a model of cyanamide molecules confined in reversed micelles, quite uniformly distributed among them and mainly located among surfactant headgroups. SAXS data analysis leads also to hypothesize a unidimensional growth of the reversed micelles with increasing the X value. Moreover, the cyanamide state and the cyanamide/cyanamide interactions in reversed micelles have been found to be different from those in pure solid cyanamide attributable to system-specific cyanamide/surfactant headgroup interactions.

Introduction

Cluster science has recently become an important trend in technology, answering the modern ever-increasing need of materials with desired specific properties. It exploits the fact that nanosized particles of certain (usually inorganic) substances exhibit novel properties that they generally do not possess in the bulk state. Moreover, the high surface-to-volume ratio that characterizes such small particles makes them very sensitive to the surrounding medium; so, their encapsulation in certain compartmentalizing structures or the adsorption of particular molecules at their surface can further influence their properties, thus opening new directions in the synthesis of material with novel properties. With this aim, the preparation of nanosized particles of a wide range of inorganic materials and their dispersion in suitable matrixes to form nanocomposites, is now a well-established strategy to prepare materials with novel physical and chemical properties of interest in modern catalysis, optoelectronics and data storage.[1−5] This strategy is based upon a wide range of synthetic protocols: vapor-phase deposition, lithography, use of biological systems, and chemical methods (sol−gel synthesis, use of aqueous solutions with or without capping agents and synthesis by means of microemulsions).

On the other hand, the compartmentalization of organic materials in microheterogeneous systems is a much less experienced but not less interesting route. For example, it has been seen that the preparation of a heterogeneously structured composite based on poly(vinyl alcohol) nanoparticles dispersed in lactic/glycolic acid polymer (PLGA) is an interesting system for long-term protein drug delivery.[6] Recently, it has been also shown that the use of solutions of reversed micelles is a good technique to solubilize small clusters of organic compounds in liquid media. The peculiar structure of the reversed micelles allows in fact the solubilization of hydrophilic substances and their dispersion as surfactant-coated clusters in apolar medium.[7−10]

The aim of the present contribution is to show the possibility of preparing stable and size-controlled molecular aggregates containing cyanamide by its solubilization in AOT/CCl_4 and lecithin/CCl_4 micellar systems. The interest in cyanamide is dictated by its use in organic synthesis as reagent (synthon) in a wide range of reactions and its effect on aldehyde dehydrogenase inhibition.[11,12] Moreover, it is worth noting that finite amounts of hydrophilic substances confined in reversed micelles can also be chemically reactive species, as already shown in a recent work.[13] In that article, the feasibility of the solid−solid reaction between nanoparticles of Na_2S and $ZnSO_4$, solubilized in the AOT micellar system to give small ZnS nanoparticles with interesting physicochemical properties has been established. Similarly, the present study can be a useful background in view of potential reactions between cyanamide and other nanosized clusters, in the confined space of reversed micelles, thus opening new directions in the interesting scenario of chemical synthesis.

Experimental Part

Materials. Sodium bis(2-ethylhexyl)sulfosuccinate (aerosol-OT, AOT, Sigma 98%) was stored in a desiccator and used after at least 1 week. In the dried AOT, a residual content of 0.2 water molecules for every surfactant molecule was found by FT-IR spectroscopy.[14] Lecithin (Degussa Bio Actives, Epicuron 200) was a generous gift of Degussa Bio Actives; cyanamide (Sigma, 99%), *n*-heptane (Aldrich, 99% spectrophotometric grade), and CCl_4 (Sigma, 99.97%) were used as received.

Methods. All samples were prepared by weight. Surfactant/apolar solvent (surfactant = AOT, lecithin; apolar solvent = *n*-heptane, CCl_4) solutions were prepared at a fixed surfactant concentration of 0.1 mol kg^{-1}. They were stirred for 30 min in the presence of P_2O_5 (Sigma, 99%) and then filtered to ensure the complete removal of residual water. It has been seen that this dehydration procedure does not chemically alter the solutions.[15,16]

Then, each cyanamide/surfactant/apolar solvent solution was prepared by adding the dried surfactant/apolar solvent solution

* Corresponding author. E-mail: turco@unipa.it.
[†] Università degli Studi di Palermo.
[‡] Istituto per lo Studio dei Materiali Nanostrutturati.

10.1021/jp0492422 CCC: $27.50
Published on Web 05/20/2004

to a weighted quantity of cyanamide to give the desired cyanamide-to-surfactant molar ratio (X). Solubilization was performed at room temperature (25 °C) and sped up by ultrasonication. Solutions were found to be stable, and no aging effects have been found within a period of several weeks.

All measurements were carried out at room temperature. SAXS patterns have been recorded by a laboratory instrumentation consisting of a Philips PW 1830 X-ray generator providing Cu Kα, Ni filtered ($\lambda = 1.5418$ Å) radiation with a Kratky small-angle camera in the "finite slit height" geometry equipped with a step scanning motor and scintillation counter. Each scattering spectrum was subtracted by the cell and solvent contributions.

IR spectra were recorded by a Bruker (IFS25) Fourier transform spectrometer using a cell equipped with CaF_2 windows. Each spectrum is an average of 100 scans collected in the frequency range 900−4000 cm^{-1} at a spectral resolution of 2 cm^{-1}.

^1H NMR spectra were collected by a Bruker AC-200 spectrometer operating at the frequency of 250.134 MHz. Spectra calibration was performed using DMSO-d_6 as an external standard.

Results and Discussion

Cyanamide solubilization in surfactant/apolar solvent solutions is itself a proof of its confinement in reversed micelles because its solubility in pure apolar solvent was found to be scarce ($\sim 10^{-3}$ M). Instead, in 0.1 mol kg^{-1} surfactant/apolar solvent systems, the thermodynamic solubility (i.e., in the presence of cyanamide crystals) was found to be $X = 1.33$ in AOT/*n*-heptane, $X = 3.00$ in lecithin/*n*-heptane, $X = 2.43$ in AOT/CCl_4, and $X = 4.30$ in lecithin/CCl_4 solutions (X = [cyanamide]/[surfactant]). Moreover, supersaturated metastable solutions can be easily prepared up to a value of $X = 2$ and $X = 3.5$ in AOT/*n*-heptane and lecithin/*n*-heptane, respectively, whereas up to a value of $X = 6$ and $X = 11$, in AOT/CCl_4 and lecithin/CCl_4, respectively. Such supersaturation effects suggest the importance of the confinement of hydrophilic substances within reversed micelles, which, owing to their peculiar structure and dynamics, can influence the nucleation process and even inhibit the crystal growth and precipitation of thermodynamically unstable samples.

To achieve structural information and to investigate the status of cyanamide confined in reversed micelles, a SAXS, FT-IR, and ^1H NMR investigation as a function of X has been carried out. The collection of SAXS spectra was performed using *n*-heptane as solvent because the high absorption coefficient of CCl_4 made the scattered intensity too low to be detected with an adequate signal-to-noise ratio. On the other hand, FT-IR and ^1H NMR spectra were performed using CCl_4 as solvent to take the advantage of its transparency on all the IR and ^1H NMR windows. It is worth noting that the CCl_4-to-*n*-heptane solvent replacement, however, involves minor changes in the micellar structure.[17−19]

SAXS Data. Typical X-ray scattering profiles of cyanamide/AOT/*n*-heptane and cyanamide/lecithin/*n*-heptane are shown in Figure 1. For comparison, the spectra of AOT/*n*-heptane and lecithin/*n*-heptane systems are also shown. Because small-angle X-ray scattering arises from the contrast in electron density between different adjacent regions and taking into account the peculiar structure of reversed micelles entrapping hydrophilic substances, the scattering centers are to be considered the hydrophilic cores of both AOT and lecithin reversed micelles.[13,20] We performed a Guinier analysis of all SAXS data

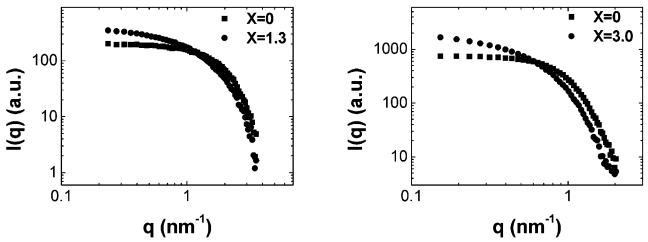

Figure 1. Typical smeared scattering profiles of AOT/*n*-heptane (left panel) and lecithin/*n*-heptane (right panel) solutions containing cyanamide at the X value shown.

to obtain the average radius of gyration (R_g) of such scattering centers as a function of X. It is worth remembering that the Guinier approximation is valid only under the condition of concentration sufficiently low so that interparticle interactions are negligible.[21] Preliminary studies, carried out as a function of surfactant concentration (i.e., micellar concentration), confirmed that at [surfactant] = 0.1 mol kg^{-1}, solutions can be considered diluted enough to allow accurate Guinier analysis. The results of all fittings are shown in Figure 2, and the derived R_g values are reported in Table 1. The linear trend of all experimental points in the $0 < q < R_g^{-1}$ range of the Guinier plot and the small residual values (Res %) confirm the validity of Guinier approximation and the absence of supramicellar aggregates. Moreover, the increase of the slope in this region as a function of X indicates an increase of R_g value with the amount of cyanamide concentration, as quantitatively shown in Table 1. This is consistent with a model of cyanamide solubilized within the micellar aggregates: the higher the amount of cyanamide confined within them, the bigger the micelles are.

However, the value of R_g itself does not provide any information about the shape of the reversed micelles; so to obtain such information, we fitted all the experimental scattering profiles with three different equations, each one considering one of the following models of noninteracting homogeneous particles:

- polydisperse spheres
- monodisperse cylinders
- monodisperse ellipsoids of rotation

In particular, when the model of polydisperse spheres was considered, we used for the scattering intensity the equation:

$$I(q) \propto \int_{-\infty}^{\infty} P(t) \int_{0}^{\infty} n(R) \cdot \phi^2(xR)\, \mathrm{d}R\, \mathrm{d}t \qquad (1)$$

where q is the elastic scattering vector, $\phi(xR)$ is the form factor of a sphere of radius R given by[21]

$$\phi(xR) = 3\left(\frac{\sin xR - xR\cos xR}{x^3R^3}\right) \qquad (2)$$

$x = (q^2+t^2)^{1/2}$, t is a variable defined along the length of the line shaped primary X-ray beam, and $P(t)$ is its intensity distribution function.[22] The integration over t takes into account the smearing effect on the experimental data due to the linear shape of the X-ray beam. The size distribution function $n(R)$ has been assumed to be the Weibull equation:[13]

$$n(R) = \left(\frac{R}{R^\circ}\right)^{b-1} \exp\left[-\left(\frac{R}{R^\circ}\right)^b\right] \qquad (3)$$

In this equation the parameter b, governing the shape of the function, is a descriptor of the size polydispersion: the lower the b value, the higher the polydispersion. R° and the mean

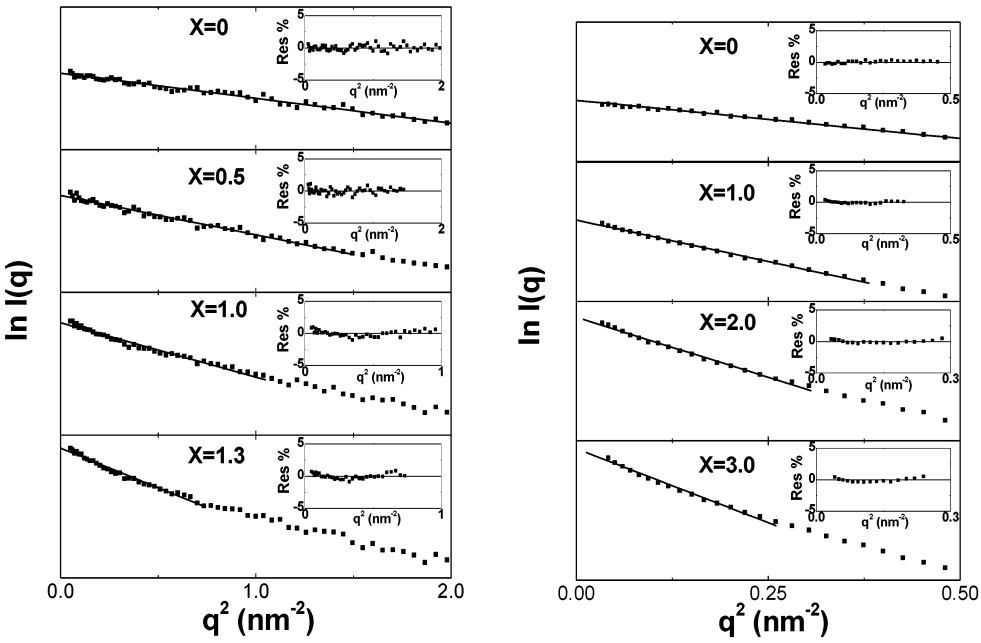

Figure 2. Plot of ln $I(q)$ vs q^2 of cyanamide/AOT/*n*-heptane (left panel) and cyanamide/lecithin/*n*-heptane (right panel) at the X values shown. The insets show the plots of the residuals.

TABLE 1: Fitting Parameters Derived from the Least-Squares Analysis of the SAXS Data of the Cyanamide/Surfactant/*n*-Heptane Systems

		Guinier analysis	polydisperse spheres			monodisperse cylinders			monodisperse ellipsoids of rotation		
surfactant	X	R_g (Å)	R_m (Å)	b	χ^2	R (Å)	h (Å)	χ^2	l_1 (Å)	l_2 (Å)	χ^2
AOT	0	8.8 ± 0.1	10.2 ± 0.1	9 ± 1	1.1	11.5 ± 0.9	17 ± 3	5.1	9.7 ± 0.13	14 ± 7	1.5
	0.5	11.2 ± 0.1	10.8 ± 0.1	6 ± 1	4.4	10.5 ± 0.4	33 ± 3	3.5	9.6 ± 0.6	22 ± 2	3.5
	1.0	13.1 ± 0.2	10.9 ± 0.1	5 ± 1	7.4	10.3 ± 0.4	51 ± 3	4.2	9.7 ± 0.3	36 ± 3	1.2
	1.3	15.8 ± 0.2	10.8 ± 0.1	3 ± 1	9.8	10.7 ± 0.7	84 ± 4	2.2	10.3 ± 0.1	48 ± 2	2.9
lecithin	0	15.8 ± 0.2	21.0 ± 0.1	26 ± 2	1.1	22 ± 2	34 ± 6	1.2	21.3 ± 0.2	22 ± 1	0.79
	1.0	23.2 ± 0.2	22.7 ± 0.1	5 ± 1	1.6	22 ± 2	62 ± 6	0.18	20.8 ± 0.4	44 ± 3	0.27
	2.0	28.1 ± 0.3	26.8 ± 0.1	6 ± 1	11	22 ± 2	130 ± 30	0.82	21.6 ± 0.1	80 ± 2	1.9
	3.0	31.7 ± 0.5	16.7 ± 0.1	1.8 ± 0.5	13	24 ± 1	174 ± 13	0.48	23.3 ± 0.3	84 ± 3	3.1

sphere radius (R_m) are correlated through the Γ function by

$$R_m = R^\circ \Gamma\left(\frac{b+1}{b}\right) \tag{4}$$

In this model the parameter b and R° were fitting parameters to be optimized.

When the model of monodisperse cylinders was considered, the equation we used was[21]

$$I(q) \propto \int_{-\infty}^{\infty} P(t) \int_0^1 \frac{J_1^2[xR(1-z^2)^{1/2}]}{[xR(1-z^2)^{1/2}]^2} \frac{\sin^2(xHz/2)}{x^2H^2z^2/4}\, dz\, dt \tag{5}$$

where J_1 is the first-order Bessel function of the first kind. R and h, being the radius and the length of the cylinder, respectively, were the parameters to be optimized by the fitting procedure.

In the model of monodisperse ellipsoids of rotation, the equation we used was[21]

$$I(q) \propto \int_{-\infty}^{\infty} P(t) \int_0^1 \phi^2 \left[xl_1 \left(1 + z^2 \left(\frac{l_2^2}{l_1^2} - 1 \right) \right)^{1/2} \right] dz\, dt \tag{6}$$

and the parameters to be optimized were the semiaxes (l_1 and l_2) of the ellipsoid of rotation. It must be noted that the number (N_{par}) of independent fitting parameters was kept constant for all models.

For each fitting procedure we considered, as probe of the goodness of the fit, the parameter χ^2 calculated as

$$\chi^2 = \frac{1}{N_{pt} - N_{par}} \sum_{i=1}^{N_{pt}} \frac{(I_{i,fit} - I_{i,exp})^2}{\sigma_i} \tag{7}$$

where each $I_{i,fit}$ is the calculated scattering intensity, $I_{i,exp}$ is the experimental scattering intensity, σ_i is the variance ($\sigma_i = \sqrt{I_{i,exp}}$), and the summation runs over all the N_{pt} experimental points. Fitting results are reported in Table 1.

Looking to the structural parameters concerning the bare reversed micelles ($X = 0$), it can be noted that (i) all models suggest a globular micellar shape and (ii) the relatively high value of the parameter b given by the model of polydisperse spheres indicates a low micellar polydispersity in agreement with the inherent monodispersion of the other two models. On the other hand, at $X > 0$, it can be noted that (i) the models of monodisperse ellipsoids and cylinders give χ^2 values lower than the model of polydisperse spheres, (ii) the micellar core length (h, $2l_2$) given by both models of cylinders and ellipsoids increases with the X value, and (iii) the micellar core cross section (R, l_1) does not increase significantly with X both in the case of AOT and in lecithin reversed micelles.

As a result of all these considerations, it can be hypothesized that there is a unidimensional growth of the reversed micelles as a function of their cyanamide content and that, at least in the range of the X values considered, the cyanamide molecules

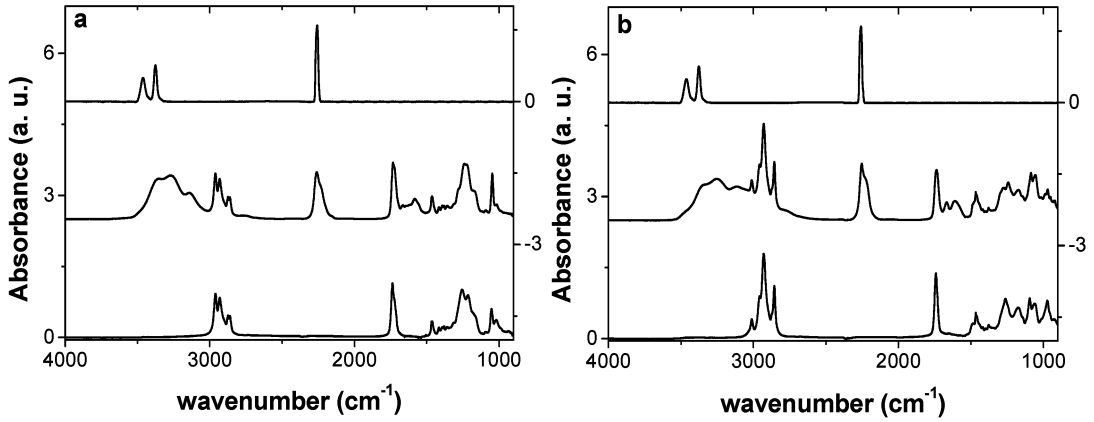

Figure 3. Infrared spectra of (a) the cyanamide/CCl_4 system (upper spectrum), cyanamide/AOT/CCl_4 system at $X = 4.76$ (intermediate spectrum), and AOT/CCl_4 system (lower spectrum), and of (b) the cyanamide/CCl_4 system (upper spectrum), cyanamide/lecithin/CCl_4 system at $X = 4.78$ (intermediate spectrum), and lecithin/CCl_4 system (lower spectrum).

TABLE 2: Infrared Frequencies of Functional Groups of Cyanamide, AOT, and Lecithin in the 900−4000 cm^{-1} Frequency Range and Their Assignments

wavenumber (cm^{-1})				
cyanamide/CCl_4	solid cyanamide	cyanamide/AOT/CCl_4	cyanamide/lecithin/CCl_4	group assignments
3462	3343	3368	3360	$\nu_{as}(NH_2)$
3376	3233	3254	3251	$\nu_s(NH_2)$
	3117	3132	3110	$2\delta(NH_2)$
			3011	ν(HC)
		2961	2958	$\nu_{as}(CH_3)$
		2932	2929	$\nu_{as}(CH_2)$
		2874	2872	$\nu_s(CH_3)$
		2861	2856	$\nu_s(CH_2)$
2260	2264, 2242	2262, 2240	2257, 2236	ν(CN)
		1735	1740	ν(CO)
		1667	1668	ν(CN) + $\delta(NH_2)$
	1572	1582	1610	$\delta(NH_2)$
		1464	1467	$\nu_{as}(CN_2) + \delta_{as}(CH_3)$ + CH_2 sciss
		1360−1390	1378	$\delta_s(CH_3) + \delta_s(CH_2)$
			1245	$\nu_{as}(PO_4^-)$
		1130−1310		$\nu_{as}(SO_3^-)$ + stretch of ester linkage
		1094	1088	CH_2 wag, CH_2 twist
			1055	δ(P−O−C), $\nu_s(PO_4^-)$
		1050		$\nu_s(SO_3^-)$

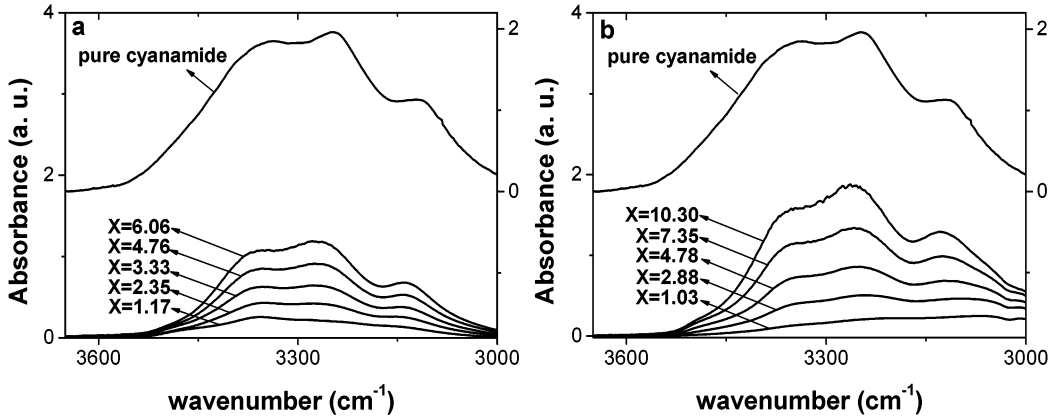

Figure 4. Comparison between the NH_2 stretching bands of solid cyanamide and those of (a) cyanamide/AOT/CCl_4 and (b) cyanamide/lecithin/CCl_4 systems at various X values.

must be located among the surfactant polar headgroups without being segregated to form a separate micellar inner core.

FT-IR Spectra. Owing to the easiness to prepare supersaturated solutions and thanks to the short time required to register a FT-IR spectrum, we were able to collect IR spectra of supersaturated solutions even up to a value of $X = 6.06$ for cyanamide/AOT/CCl_4 and $X = 10.3$ for cyanamide/lecithin/CCl_4 much before the solutions underwent phase separation.

Typical spectra of cyanamide/AOT/CCl_4 and cyanamide/lecithin/CCl_4 systems in the frequency range 900−4000 cm^{-1} are shown in Figure 3. In this figure, the spectra of cyanamide/CCl_4, AOT/CCl_4, and lecithin/CCl_4 systems are also shown for comparison. All the observed bands can be attributed to the functional groups of cyanamide, AOT, and lecithin and their assignments are shown in Table 2. Of particular interest are the cyanamide NH_2 (3000−3500 cm^{-1}) and CN (about 2260

TABLE 3: Single Component Parameters (Position/Width/Area[a]) Obtained by Deconvolution of the NH Stretching Band in the 3000−3600 cm^{-1} Frequency Region

	Pure Cyanamide	
3343/187/66	3233/74/13	3117/107/21
	Cyanamide/AOT/CCl_4	
	$X = 1.17$	
3370/98/40	3255/121/44	3138/91/16
	$X = 1.61$	
3368/109/43	3252/107/39	3136/83/18
	$X = 2.35$	
3367/108/42	3251/107/40	3133/82/18
	$X^b = 2.97$	
3368/108/43	3252/104/40	3132/81/17
	$X^b = 3.33$	
3368/112/43	3252/102/39	3132/81/18
	$X^b = 4.13$	
3369/111/42	3252/102/40	3131/80/18
	$X^b = 4.76$	
3368/110/42	3254/99/39	3132/82/19
	$X^b = 6.06$	
3369/109/41	3255/98/40	3131/83/19
	Cyanamide/Lecithin/CCl_4	
	$X = 1.03$	
3360/93/13	3248/127/42	3111/125/45
	$X = 2.88$	
3360/93/22	3248/116/40	3111/122/38
	$X^b = 4.78$	
3360/93/25	3251/106/38	3110/121/37
	$X^b = 7.35$	
3363/97/29	3250/105/40	3112/106/31
	$X^b = 10.30$	
3365/95/29	3252/108/43	3114/100/28

[a] Position (cm^{-1}), width (cm^{-1}), area (%). [b] Thermodynamically unstable samples.

TABLE 4: Single Component Parameters (Position/Width/Area[a]) Obtained by Deconvolution of the CN Stretching Band

Pure Cyanamide	
2264/22/17	2238/59/83
Cyanamide/AOT/CCl_4	
$X = 1.17$	
2261/26/33	2240/55/67
$X = 1.61$	
2262/28/33	2238/60/67
$X = 2.35$	
2263/27/30	2238/56/70
$X^b = 2.97$	
2264/25/27	2239/55/73
$X^b = 3.33$	
2264/24/26	2240/55/74
$X^b = 4.13$	
2265/24/25	2240/56/75
$X^b = 4.76$	
2265/23/23	2241/56/77
$X^b = 6.06$	
2265/22/22	2241/55/78
Cyanamide/Lecithin/CCl_4	
$X = 1.03$	
2248/24/43	2220/33/57
$X = 2.88$	
2256/20/20	2228/51/80
$X^b = 4.78$	
2256/18/18	2232/54/82
$X^b = 7.35$	
2258/18/17	2235/56/83
$X^b = 10.30$	
2260/15/16	2238/55/84

[a] Position (cm^{-1}), width (cm^{-1}), area (%). [b] Thermodynamically unstable samples.

cm^{-1}) stretching bands, due to the surfactant alkyl chain CH (2800−3000 cm^{-1}) stretch and the typical bands of the surfactant functional groups: the SO_3^- of the AOT (symmetric stretch at 1080−1020 cm^{-1}) and the PO_4^- of lecithin (antisymmetric stretch at 1320−1200 cm^{-1}).

The CH (2800−3000 cm^{-1}) stretching band is a good probe of the state of surfactant alkyl chains because it is sensitive to their lateral packing order and conformational dynamics.[23,24] It has been observed that no significant change on the band shape, position, and intensity occurs as a function of X, indicating that cyanamide confinement in AOT and lecithin reversed micelles does not significantly modify the structure and dynamics of the micellar hydrophobic layer.

Concerning the cyanamide NH_2 stretching band, it is worth noting that cyanamide dissolved in pure CCl_4 gives two sharp bands at 3376 and 3462 cm^{-1}, respectively. According to the literature, they were attributed, respectively, to the symmetric and antisymmetric NH_2 stretching vibrations of monomerically dispersed cyanamide.[24,25]

On the other hand, the NH_2 stretching band of solid cyanamide, which is shown in Figure 4, appears to be broad and red-shifted by about 130 cm^{-1} with respect to that of cyanamide dissolved in CCl_4. Deconvolution of this band

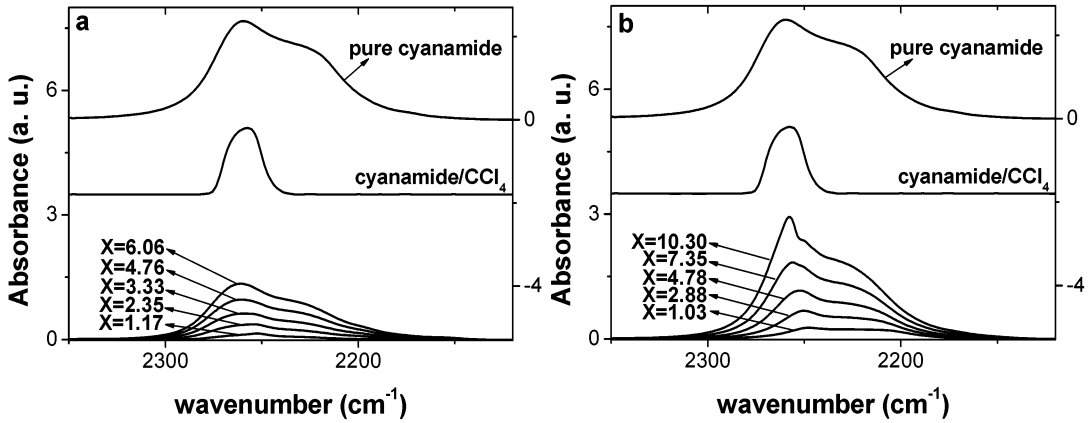

Figure 5. CN stretching bands of cyanamide in the solid state, in cyanamide/CCl_4 solution, and in (a) the cyanamide/AOT/CCl_4 system or (b) the cyanamide/lecithin/CCl_4 system at various X values.

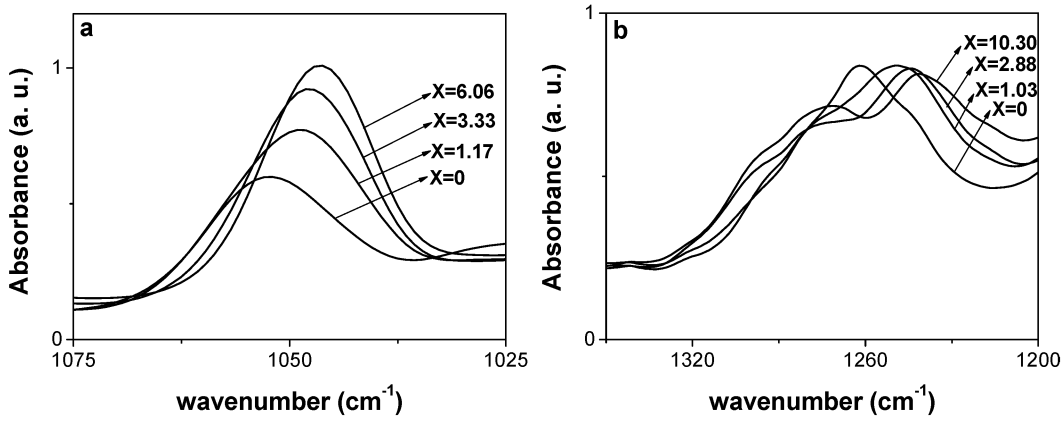

Figure 6. (a) SO_3^- symmetric stretching band of the cyanamide/AOT/CCl_4 system and (b) PO_4^- antisymmetric stretching band of cyanamide/lecithin/CCl_4 system at various *X* values.

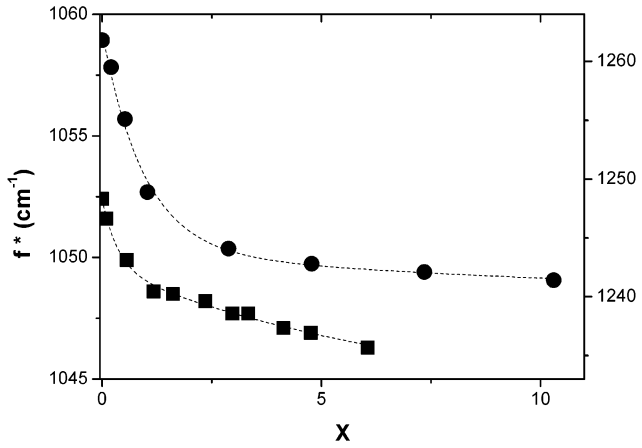

Figure 7. Peak frequency (*f**) of the SO_3^- symmetric stretching band of the cyanamide/AOT/CCl_4 system (■, left scale) and of the PO_4^- antisymmetric stretching band of the cyanamide/lecithin/CCl_4 system (●, right scale) as a function of *X*.

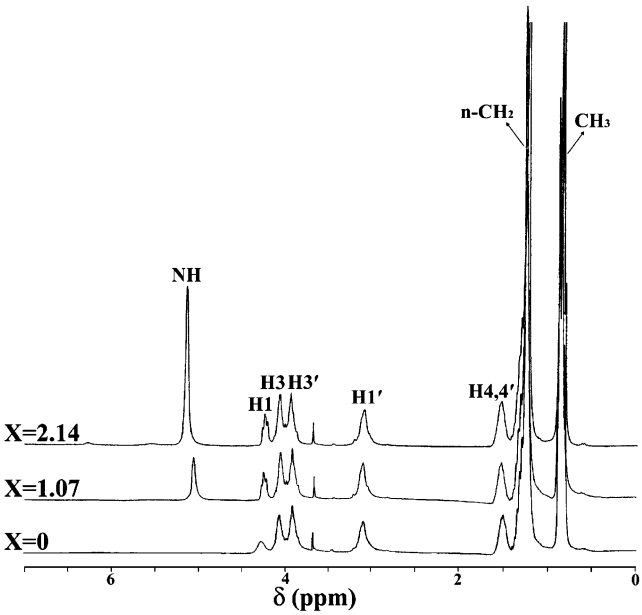

Figure 8. Comparison between ^{1}H NMR spectra of the cyanamide/AOT/CCl_4 system at various *X* values.

showed that it is well-described by three broad Gaussian components occurring at 3117, 3233, and 3343 cm^{-1}. Considering that H-bonding broadens the NH_2 stretching bands and shifts them toward lower frequencies, the 3233 and 3343 cm^{-1}

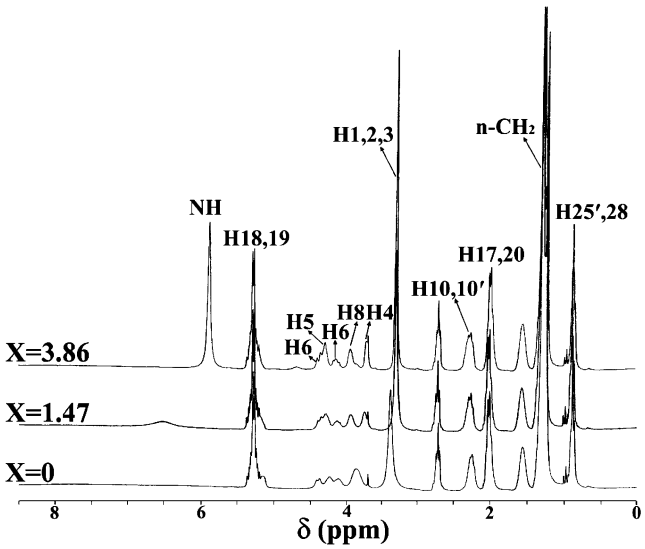

Figure 9. Comparison between ^{1}H NMR spectra of the cyanamide/lecithin/CCl_4 system at various *X* values.

TABLE 5: Chemical Shift of Cyanamide and AOT Protons in the Cyanamide/AOT/CCl_4 System as Function of *X*

cyanamide	AOT						
NH	H1	H1′	H3	H3′	H4,4′	*n*-CH_2	CH_3
			$X = 0$				
	4.27	3.10	4.06	3.91	1.53	1.26	0.89, 0.86
			$X = 0.50$				
4.99	4.26	3.10	4.06	3.92	1.54	1.26	0.89, 0.86
			$X = 1.07$				
5.07	4.26	3.10	4.06	3.93	1.54	1.27	0.89, 0.87
			$X = 2.14$				
5.12	4.26	3.09	4.06	3.93	1.55	1.27	0.89, 0.87

components can be attributed, respectively, to symmetric and antisymmetric NH_2 stretching vibrations of H-bonded cyanamide molecules, whereas, according to the literature, the 3117 cm^{-1} component can be assigned to the $2\Sigma(NH_2)$ overtone.[26] The NH_2 stretching band of the cyanamide confined in reversed micelles, compared with that of the pure solid cyanamide, is also reported in Figure 4 as a function of the *X* value for both surfactants. Only minor changes of the band position, shape, and width with respect to pure cyanamide are observed. This finding indicates that cyanamide NH_2 groups in surfactant/CCl_4 solutions are mainly confined in the hydrophilic domain of reversed micelles forming strong H-bonds.

To gain more information, the NH_2 bands were analyzed in terms of Gaussian components. A deconvolution procedure

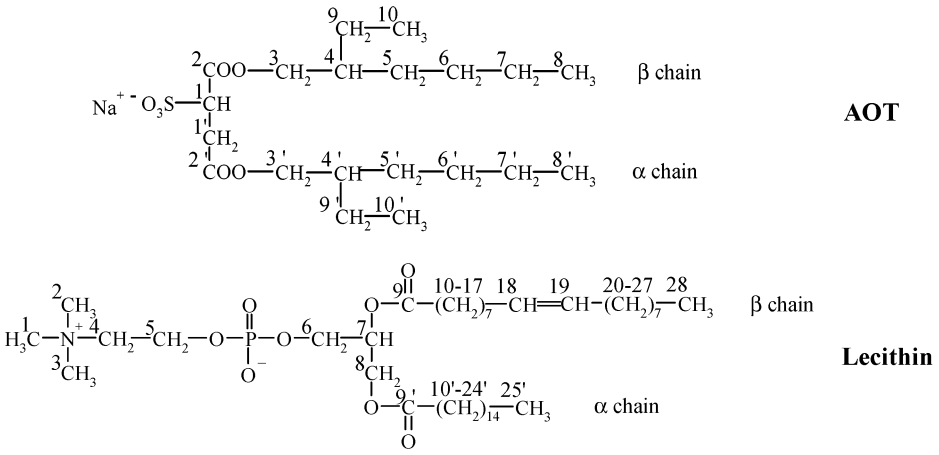

Figure 10. Molecular structures and atom numbering of AOT and lecithin.

TABLE 6: Chemical Shift of Cyanamide and Lecithin Protons in the Cyanamide/Lecithin/CCl_4 System as Function of *X*

cyanamide	lecithin									
NH	H18,19	H4	H5	H6	H8	H1−3	H10,10′	H17,20	*n*-CH_2	H25′,28
					$X = 0$					
	5.26	3.82	4.27	4.09, 4.35	3.90	3.35	2.24	2.00	1.30	0.88
					$X = 0.53$					
6.99	5.25	3.76	4.22	4.12, 4.33	3.88	3.32	2.24	2.00	1.29	0.89
					$X = 1.47$					
6.52	5.25	3.71	4.25	4.10, 4.32	3.91	3.28	2.25	2.00	1.29	0.89
					$X = 3.86$					
5.87	5.25	3.69	4.27	4.12, 4.33	3.91	3.28	2.27	2.00	1.30	0.89

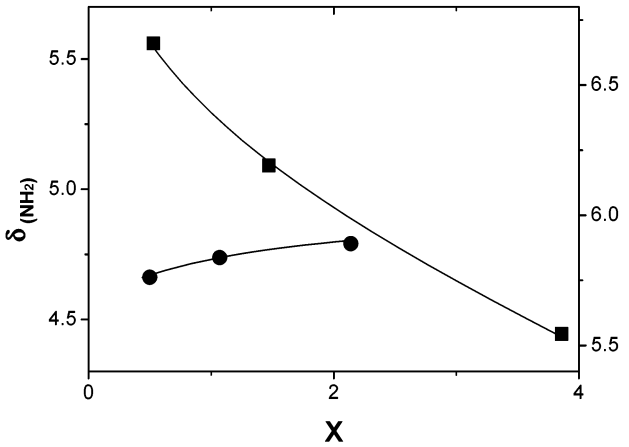

Figure 11. Cyanamide NH chemical shifts for the cyanamide/AOT/CCl_4 system (●, left scale) and for the cyanamide/lecithin/CCl_4 system (■, right scale) as a function of *X*.

showed that all bands can be well described by three Gaussian curves centered at about 3132, 3254, and 3368 cm^{-1} for cyanamide in AOT/CCl_4 and at about 3110, 3251, and 3360 cm^{-1}, for cyanamide in lecithin/CCl_4 solutions. The fitting parameters of these components, together with those of pure solid cyanamide, are reported in Table 3. Because the three components show minor position changes with respect to those of pure cyanamide, they can be assigned to the same vibration modes, respectively.

With regard to the position of the components attributed to the symmetric and antisymmetric NH_2 vibrations of confined cyanamide molecules, it seems that they are not influenced by *X* and are scantily affected by the surfactant nature. Because these positions are blue shifted by about 20 cm^{-1} with respect to those observed in pure cyanamide, it can be also argued that the encapsulation of cyanamide in AOT and lecithin reversed micelles involves a limited weakening of the H-bond strength. Moreover, a comparison with the band of pure cyanamide reveals that the area and width of these components show some surfactant-dependent changes. Taking into account that the area of an absorption band is influenced by the variation of the molecular dipole moment with the normal coordinate ($\partial\mu/\partial q$), the surfactant-specific area changes suggest that these quantities are differently perturbed by micellar confinement. This effect could originate from the substitution of cyanamide−cyanamide hydrogen bonds with cyanamide−surfactant headgroup interactions. On the other hand, the changes in the component widths can be attributed to variation of the relative populations of differently H-bonded cyanamide molecules. Because spectral differences between confined and bulk cyanamide are observed even at the higher *X* values including the thermodynamically unstable samples, it can be inferred that in both micellar systems cyanamide NH_2 groups are always quite homogeneously distributed among the reversed micelles and most probably located, opportunely oriented, within the hydrophilic surfactant headgroup domain.

Concerning the environment probed by the cyanamide CN groups, specific information can be derived through a perusal of Figure 5. This figure reports the CN stretching band of the pure solid cyanamide, cyanamide in CCl_4, and cyanamide confined in reversed micelles at various *X* values for both surfactants. It can be noted that, in contrast with the CN stretching vibration of cyanamide in CCl_4 solution characterized by a single peak (2260 cm^{-1}), the bands of solid and confined cyanamide are broader and show a shoulder at the lower frequency side. According to the literature, these bands have been analyzed in terms of two Gaussian components:

(i) a higher frequency component centered at about 2260 cm^{-1} due to CN groups soaked in a quite apolar environment and

(ii) a lower frequency one centered at about 2236 cm^{-1} attributable to those surrounded by hydrophilic groups.[27]

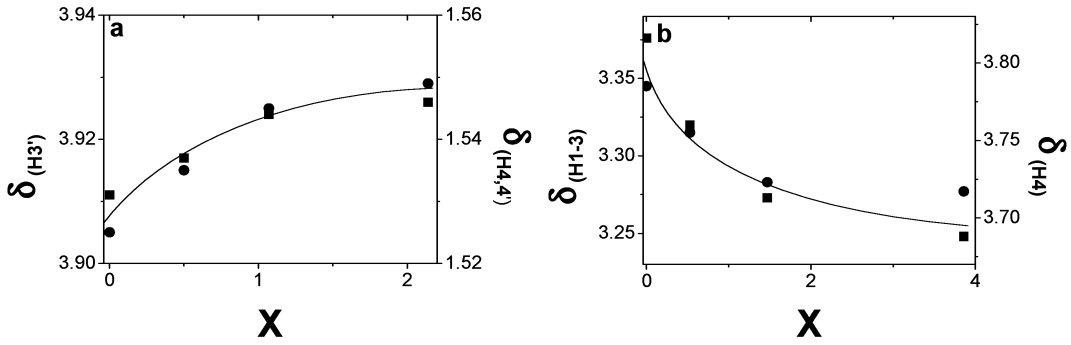

Figure 12. Chemical shifts of some representative protons of (a) the cyanamide/AOT/CCl_4 system (●, δ_{H3}; ■, $\delta_{H4,4'}$) and of (b) the cyanamide/lecithin/CCl_4 system (●, δ_{H1-3}; ■, δ_{H4}) as a function of *X*.

The results of this analysis are shown in Table 4. It can be noted that the area of the lower frequency component increases with *X*, tending to the value of solid cyanamide. This finding suggests that increasing *X* causes a parallel increase of the fraction of CN groups located within surfactant headgroups. This implies that, by adding cyanamide, a progressive rearrangement of the hydrophilic domain formed by cyanamide and surfactant headgroups occurs.

The SO_3^- symmetric stretching and the PO_4^- antisymmetric stretching bands are shown in Figure 6 as a function of *X*. It can be seen that in both cases a progressive shift toward lower frequencies with *X* occurs, revealing the presence of specific interactions between cyanamide and the surfactant polar heads. Considering the conclusions derived from the inspection of Figures 4 and 5, a direct interaction between the surfactant polar head and the cyanamide NH and CN groups is likely to take place. Moreover, an increase of the SO_3^- peak intensity in the case of AOT must be noted. Considering the fact that the intensity of an absorption band is proportional to the variation of the molecular dipole moment with the normal coordinate, this effect suggests a progressive polarization of the headgroup as a consequence of the increase of the number of confined cyanamide molecules. This effect, instead, does not occur in the PO_4^- antisymmetric stretching band of the lecithin, which is practically *X*-insensitive. In this case, the interactions between the polar head of lecithin and cyanamide do not cause significant variations in the dipole moment of the PO_4^- group.

Figure 7 reports the frequencies of the maxima of absorption (f^*) of the AOT SO_3^- symmetric stretching and of the lecithin PO_4^- antisymmetric stretching as a function of *X*. One can note a first and steep decrease of these values followed by a plateau. This trend is similar to that already observed in water/AOT liquid crystals and water/AOT/CCl_4 microemulsions[28] and indicates a progressive increase of the fraction of hydrophilic surfactant headgroups interacting with cyanamide and, in the plateau region, the saturation of surfactant headgroups.

Further comments can be made:

•There is no significant difference between the spectral features of the thermodynamically stable ($X < 2.43$ for AOT/CCl_4 and at $X < 4.30$ for lecithin/CCl_4 solutions) and unstable (supersaturated) samples.

•Even at the higher *X* values (comprising the supersaturated samples) the spectral features of confined cyanamide are different from those of pure cyanamide.

These observations suggest that, in supersaturated samples, no marked variation of the confined cyanamide state occurs with respect to the unsaturated ones and that the cyanamide molecules undergo confinement effects pointing out the important role played by the surfactant in stabilizing, through the formation of specific interactions, small cyanamide/surfactant headgroup clusters.

^{1}H NMR Spectra. Typical ^{1}H NMR spectra of cyanamide/AOT/CCl_4 and cyanamide/lecithin/CCl_4 systems are compared to those of AOT/CCl_4 and lecithin/CCl_4 in Figures 8 and 9, respectively. In these figures one can note the presence of the unique peak due to the amino group in cyanamide and the peaks due to AOT and lecithin protons, whose assignment was made according to the literature.[29,30] Atom numbering of AOT and lecithin is shown in Figure 10.

Tables 5 and 6 report the positions of the various peaks. An inspection of these data leads us to some observations:

•The position of the peak of NH_2 protons of the cyanamide in AOT is different from that in lecithin.

•The peak of NH_2 protons of the cyanamide confined in AOT varies upfield by increasing the *X* value, whereas it varies downfield in the case of lecithin (see Figure 11).

•There is a progressive shift of the peaks of some surfactant protons close to the polar headgroups with *X*. Some of them (H3′ and H4,4′ in AOT) shift downfield, and others (H1−3 and H4 in lecithin) shift upfield (see Figure 12).

These findings are consistent with the hypothesis that the progressive addition of the cyanamide molecules among the surfactant headgroups involves a progressive change of the electron cloud density around the protons of cyanamide and those of the surfactant alkyl chains close to the polar headgroups. These observations confirm the occurrence of a direct and specific interaction of the cyanamide NH_2 with the different polar headgroups of the two surfactants and suggest a progressive structural variation of the core of AOT and lecithin reversed micelles with *X*.

Conclusions

This study shows that simple solubilization of cyanamide in AOT/CCl_4 or in lecithin/CCl_4 micellar solutions leads to the entrapment of cyanamide molecules within reversed micelles, quite uniformly distributed among them and involving a unidirectional growth of reversed micelles with the cyanamide-to-surfactant ratio. The confined cyanamide molecules are, as highlighted by the coupled IR and ^{1}H NMR investigations, opportunely oriented and strongly interacting with the surfactant polar headgroups, preserving, however, the lateral packing structure of the surfactant chains. Due to these peculiar cyanamide−surfactant interactions, long-living (several hours) supersaturated cyanamide solutions, even up to about 3 times the thermodynamic solubility, can be prepared. These long-living systems together with stable samples can be very interesting

candidates for novel organic solid-state reactions in the confined space of reversed micelles.

Acknowledgment. Financial support from MIUR 60% is gratefully acknowledged.

References and Notes

(1) Haglund, R. F., Jr. *Mater. Sci. Eng. A* **1998**, *253*, 275.
(2) Bhargava, R. N.; Gallagher, D.; Welker, T. *J. Lumin.* **1994**, *275*, 60.
(3) Litvinov, D.; Khizroev, S. *Nanotechnology* **2002**, *13*, 179.
(4) Pileni, M. P. *Nature Mater.* **2003**, *2*, 145.
(5) Pileni, M. P. *J. Phys. Chem. B* **2001**, *105*, 3358.
(6) Wang, N.; Wu, X. S.; Li, J. K. *Pharm. Res.* **1999**, *16(9)*, 1430.
(7) Ruggirello, A.; Turco Liveri, V. *Chem. Phys*. **2003**, *288*, 187.
(8) Debuigne, F.; Jeunieau, L.; Wiame, M.; Nagy, J. B. *Langmuir* **2000**, *16*, 7605.
(9) Sen, S.; Sukul, D.; Dutta, P.; Bhattacharyya, K. *J. Phys. Chem. B* **2002**, *106*, 3763.
(10) Moulik, S. P.; De, G. C.; Bhowmik, B. B.; Panda, A. K. *J. Phys. Chem. B* **1999**, *103*, 7122.
(11) Hammond, A. H.; Fry, J. R. *Chem.-Biol. Interact.* **1999**, *122*, 107.
(12) Falgueyret, J. P.; Oballa, R. M.; Okamoto, O.; Wesolowski, G.; Aubin, Y.; Rydzewski, R. M.; Prasit, P.; Riendeau, D.; Rodan, S. B.; Percival, M. D. *J. Med. Chem.* **2001**, *44*, 94.
(13) Calandra, P.; Longo, A.; Turco Liveri, V. *J. Phys. Chem. B* **2003**, *107*, 25.
(14) Arcoleo, V.; Goffredi, M.; Turco Liveri, V. *J Colloid Interface Sci.* **1998**, *198*, 216.
(15) Temsamani, M. B.; Haeck, M.; El Hassani, I.; Hurwitz, H. D. *J. Phys. Chem. B* **1998**, *102*, 3335.
(16) Calvaruso, G.; Ruggirello, A.; Turco Liveri, V. *J. Nanopart. Res.* **2002**, *4*, 239.
(17) Riter, R. E.; Kimmel, J. R.; Undiks, E. P.; Levinger, N. E. *J. Phys. Chem.* **1998**, *102*, 7931.
(18) Bhattacharyya, K. *Acc. Chem. Res.* **2003**, *36*, 95.
(19) Levinger, N. E. *Curr. Opin. Colloid Interface Sci.* **2000**, *5*, 118.
(20) Mackeben, S.; Müller-Goymann, C. C. *Int. J. Pharm.* **2000**, *196*, 207.
(21) Feign, L. A.; Svergun, D. I. *Structure Analysis by Small-Angle X-ray and Neutron Scattering*; Plenum Press: New York, 1987.
(22) Ruland, W. *J. Appl. Crystallogr.* **1974**, *7*, 383.
(23) Edwards, W. L.; Bush, S. F.; Mattingly, T. W.; Weisgraber, K. H. *Spectrochim. Acta, Part A* **1993**, *43*, 2027.
(24) Calvaruso, G.; Minore, A.; Turco Liveri, V. *J. Colloid Interface Sci.* **2001**, *243*, 227.
(25) Ruggirello, A.; Turco Liveri, V. *Colloid Polym. Sci.* **2003**, *281*, 1062.
(26) Iogansen, A. V.; Kurkchi, G. A.; Dementijeva, L. A. *J. Mol. Struct.* **1976**, *35*, 101.
(27) Barthel, J.; Buchner, R.; Wismeth, E. *J. Solution Chem.* **2000**, *29*, 937.
(28) Calandra, P.; Caponetti, E.; Chillura Martino, D.; D'Angelo, P.; Minore, A.; Turco Liveri, V. *J. Mol. Struct*. **2000**, *522*, 165.
(29) Heatley, F. *J. Chem. Soc., Faraday Trans. 1* **1987**, *83*, 517.
(30) Capitani, D.; Segre, A. L.; Dreher, F.; Walde, P.; Luisi, P. L. *J. Phys. Chem.* **1996**, *100*, 15211.